ISSN 0915-633X

NATIONAL INSTITUTE FOR FUSION SCIENCE

Field Line and Particle Orbit Analysis in the Periphery of the Large Helical Device

Y. Matsumoto, S.-I. Oikawa and T. Watanabe

(Received - Aug. 23, 2001)

NIFS-713 Sep. 2001

RESEARCH REPORT
NIFS Series

TOKI, JAPAN

Field line and Particle orbit Analysis in the Periphery of the Large Helical Device

Yutaka MATSUMOTO,* Shun-ichi OIKAWA, and Tsuguhiro WATANABE[1]

Graduate School of Engineering, Hokkaido University, Sapporo 060-8628, JAPAN
[1]National Institute for Fusion Science, Toki 509-5292, JAPAN

*e-mail: shopon@fusion.qe.eng.hokudai.ac.jp

Keywords: LHD, peripheral plasma, chaotic field line, particle orbit, potential control

Abstract:

Magnetic field lines and particle orbits are analyzed in the periphery of the Large Helical Device (LHD), which is called chaotic field line region. The inner and outer borders of the chaotic field line region are determined precisely. It is found that the particles confined in the chaotic field line region are classified into two groups that are passing particles and reflected particles. Passing particles have long lifetime, because of the long connection length of the chaotic field line. Reflected particles are confined because they are trapped by the magnetic mirror in the chaotic field line region due to the strong adiabaticity. There exist the exceptional particles among the reflected particles. The mechanisms of the exceptional particles are described by the analysis of the magnetic structure in the chaotic field line region. The precise comparison between $R_{\rm ax} = 3.75$ m and $R_{\rm ax} = 3.6$ m magnetic configuration is carried out.

1 Introduction

The confinement of particles is of great importance in the research of helical devices, such as the Large Helical Device (LHD) at the National Institute for Fusion Science (NIFS) in Japan. LHD, the largest helical device in the world, uses superconducting magnets with $\ell/m = 2/10$, $R/a \simeq 3.9$ m/0.6 m and $B_0 \simeq 3$ T heliotron type magnetic field configuration with no toroidal coils [1]. The specification of LHD is shown in Table 1 for references.

Table 1: Specification of LHD [1].

Major radius R	3.9 m
Minor radius a	0.6 m
Plasma volume	20-30 m^3
Toroidal mode number m	10
Poloidal mode number ℓ	2
B_0 ($\|\boldsymbol{B}\|$ on magnetic axis)	3 T

In helical devices, particles are usually classified into three groups called passing particles, blocked particles and localized particles [2]. The blocked particles trapped in the toroidal magnetic ripple are thought to cause the deterioration of plasma confinement in toroidal machines. Especially, in the helical machines, the localized particle trapped in the helical magnetic ripple have been believed to be extremely harmful to plasma confinement, because the rotational transform cannot cancel the toroidal drift of these particles and so these particles are eventually lost to the vacuum vessel wall [3, 4].

In the analysis of the high energy particles which are produced by the perpendicular Neutral Beam Injection (NBI) in Heliotron E, Hanatani et al. [5] have been found that most of localized particles are confined in Heliotron E and that the high heating efficiency is obtained because there exists re-entering particles in $\ell = 2$ heliotron configurations. On the other hand, in the particle orbit analysis in $\ell = 2$ helical device such as LHD, it has been reported that there exists the large loss region in the velocity space and that reflected particles (blocked particles and localized particles) which have small $v_\parallel$ are lost to the outside the Last Closed Magnetic Surface (LCMS) [6]. The difference of the conclusions for the localized particles confinement is due to the difference of the assumption for the particle loss boundary. Fowler et al. [7] have pointed out that the treatment of the loss boundary is very important in the particle orbit analysis in helical systems and that the orbit loss is decreased about 30 % when the loss boundary is set at vacuum vessel wall. Watanabe et al. [8] have also pointed out the importance of the loss boundary and found that almost all reflected particles show the

good confinement characteristics in LHD.

The objects of these studies have mostly been just the core plasma [5, 7, 8]. In order to achieve the high plasma confinement, however, the peripheral plasma plays the following important roles:

- to protect the core plasma from the cooling down by neutrals outside the plasma.
- to reduce the heat load to the divertor plate without losing high-performance core plasma confinement.

Therefore, it is important to study the plasma behavior in the periphery of LHD, and to confirm whether the peripheral plasma of LHD can play these important roles. Thus, we analyze the particle orbit traced from the outside of the LCMS. In the peripheral region, passing particles would have the finite lifetime, since the magnetic field lines reach the wall. Reflected particles, on the other hand, are likely to be confined in the peripheral region. The purpose of the present paper is to show characteristics of the particle orbits in the peripheral region of LHD due to the strong adiabaticity for the reflected particles [9] and to indicate that the particles can actually play important and useful roles in the region outside the LCMS.

In LHD, there exists a magnetic field line region usually called the ergodic or the stochastic region. Because there are many magnetic islands in the peripheral region of LHD, this region cannot be expressed in "ergodic". We cannot call this region "the stochastic region", since this region is not controlled by some stochastic processes but controlled by a simple Hamiltonian system. So, in this paper, we call this field line region the chaotic field line region. Akao [10] has reported the detailed structure of the peripheral region in LHD. It has been shown that there exist the three different regions: the chaotic region near the LCMS, the whisker region, and the inter-whisker region outside the chaotic region. In the chaotic field line region, field lines exhibit chaotic behavior and have long connection lengths. Whisker field lines regularly repeat three processes: stretching, folding, and nesting or they exhibit irregular behaviors. As a result of such processes, whisker field lines have long connection lengths. Inter-whisker field lines have short connection lengths and they exhibit only regular behavior. Although behaviors of chaotic field lines have been clarified, the magnetic field used in Akao's paper is slightly different from the magnetic field in actual LHD. Moreover, the quantitative analysis of chaotic field lines has not been done. Thus, it is the second purpose of this paper to analyze the magnetic field lines in the peripheral region of LHD with the actual vacuum magnetic field and to clarify the borders of the chaotic field line region. The connection lengths of chaotic field lines are also studied precisely.

LHD can be operated in the various positions of the magnetic axis, which is placed at $R_{ax} = 3.75$m in the standard magnetic configuration, by controlling the current of coils. As the results of the recent experiments of LHD, it is reported that the plasma confinement is improved by the inward shift of the magnetic axis to $R_{ax} = 3.6$ m [11]. We study the difference between these magnetic configurations in regard to the magnetic field structure and the particle orbit. And we clarify the reason of the improvement of the plasma confinement in $R_{ax} = 3.6$ m configuration.

The results of the field line tracing in the chaotic field line region are shown in §2. In §3 the particle orbit in the chaotic field line region is described. Section 4 is devoted to summary and discussion.

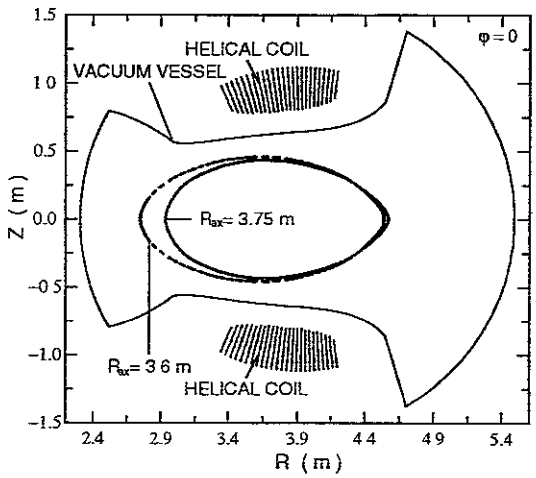

Figure 1: Poincare plot of the Last Closed Magnetic Surface (LCMS) in LHD at the toroidal angle $\varphi = 0$. The toroidal angle $\varphi = 0$ denotes the horizontally elongated poloidal plane in LHD. Gray points represent the LCMS in the $R_{ax} = 3.75$ m configuration. Black points denote the LCMS in the $R_{ax} = 3.6$m configuration. The vacuum vessel wall and helical coils of LHD are also shown.

2 Field Line Tracing in the Chaotic Field Line Region

The inner border of the chaotic field line region is the LCMS. In order to determine the position of the LCMS, we sweep the starting points of the field line trace on the line ($\varphi = 0$, $Z = 0$). The position of the LCMS is numerically determined by the field line tracing during 20,000 circulations in the magnetic field direction and the opposite direction. In the case of $R_{ax} = 3.75$ m, the position of the LCMS is found at $R = 4.5732$ m for the step size of scanning $\delta R = 10^{-4}$ m. The position of the LCMS is also found at $R = 4.5405$ m in the case of $R_{ax} = 3.6$ m.

As depicted in Fig. 1, the core plasma region (inside the LCMS) of $R_{ax} = 3.75$ m configuration is slightly smaller than that of $R_{ax} = 3.6$ m configuration

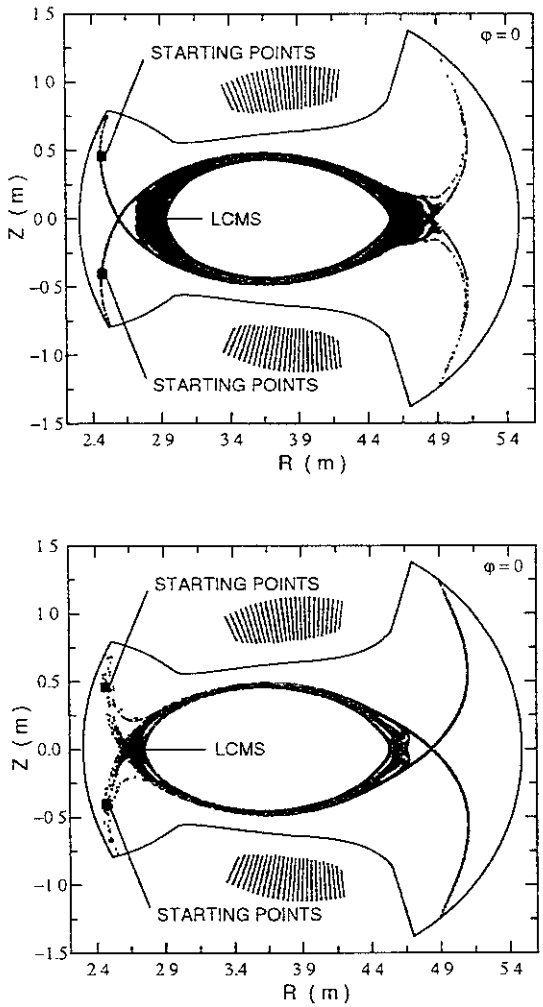

Figure 2: Poincare plot of the divertor field lines at the toroidal angle $\varphi = 0$ in the case of $R_{ax} = 3.75$ m(a) and $R_{ax} = 3.6$ m(b). Black points represent the LCMS. Gray points denote the region through which divertor field lines have passed. Starting points are shown for references.

Chaotic field lines reach the divertor plate after a lot of circulation around the torus. So in order to determine the outer boundary of the chaotic field line region, the field lines are traced from the starting points outside the LCMS and make Poincare plots excluding the field lines the connection length of which are shorter than 5 toroidal turns. The outer boundaries of the chaotic field line region on $\varphi = 0$ are summarized in Table 2 in which the widths of the chaotic field line region Δ_{chaos} are also shown. It is seen from Table 2 that the chaotic field line region of $R_{ax} = 3.75$ m configuration is thicker than that of $R_{ax} = 3.6$ m in the outside the torus.

Table 2: Outer boundaries of the chaotic field line region.

$R_{ax} = 3.75$ m			$R_{ax} = 3.6$ m		
R	Z	Δ_{chaos}	R	Z	Δ_{chaos}
3.7500	0.4698	0.0325	3.6000	0.4671	0.0097
3.7500	-0.4743	0.0370	3.6000	-0.4671	0.0097
4.7891	0.0000	0.2159	4.6398	0.0000	0.0993
2.7293	0.0000	0.1897	2.6154	0.0000	0.1395

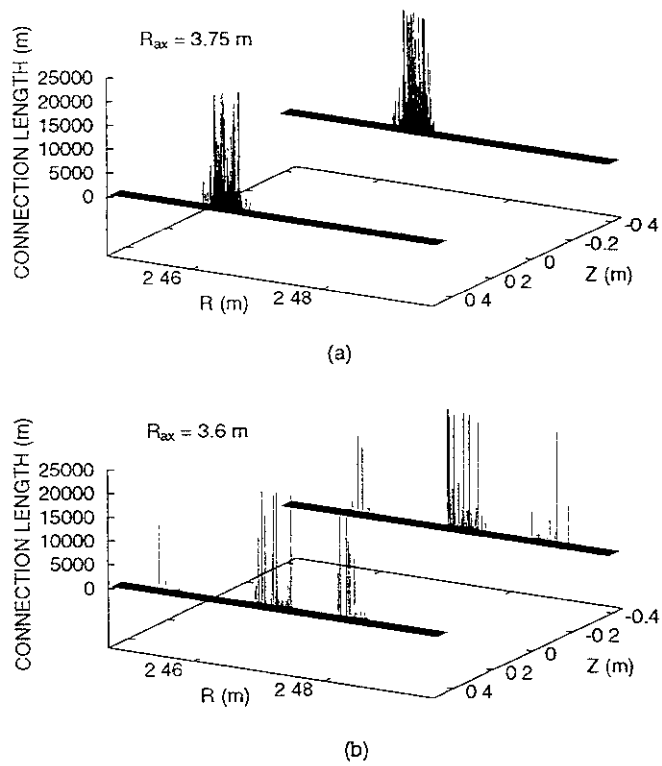

Figure 3: Connection lengths of the divertor field lines which are traced from the positions near the divertor plate to the plasma core in the case of $R_{ax} = 3.75$ m(a) and $R_{ax} = 3.6$ m(b).

In order to confirm above results, divertor field lines are traced from positions on the divertor plate ($\varphi \simeq 0$) toward the plasma region as shown in Fig. 2. The determined LCMS coincides with the inner border of Poincare plots of the divertor field line tracing. It is also seen that divertor field lines spread out as far as the determined outer boundary of the chaotic field line region.

Figure 3(a) shows the connection lengths of the divertor field lines which are traced from the positions equal to Fig. 2 in the $R_{ax} = 3.75$ m magnetic field. The longest

connection length of the divertor field line is up to almost 20 km. The connection lengths of divertor field lines are long compared to tokamaks in which the connection length of divertor field line is almost 100 m [12]. Although such long field lines can approach the core region, short field lines cannot approach the core. In other words, the chaotic field lines that are traced from the chaotic field line region to the divertor plate have sufficiently long connection lengths. Especially, the chaotic field lines passing through near the LCMS have long connection lengths, as shown by Akao [10].

Similarly, the connection lengths of divertor field lines are also long in the case of $R_{ax} = 3.6$ m. It is seen from Fig. 3(b) that there are three peaks of the connection length in $R_{ax} = 3.6$ m configuration corresponding to the whisker field lines as shown in Fig 2.

3 Particle Orbit in the Chaotic Field Line Region

Usually, particles orbit in helical devices have been classified into the groups: passing particles, localized particles and blocked particles [2]. However, it would not be suitable to discuss the particle orbit with such a classification, because the transition between the localized particles and the blocked particles is possible without collisions. In this paper, we classify the particle orbits in LHD into the passing particles and the reflected particles. The reflected particles include both the non-chaotic orbit particles and the chaotic orbit particles. The non-chaotic orbit particles traced from the core plasma region make the clear drift surface on Poincare plots. The chaotic orbit particles are the particles that repeatedly transit between the localized orbit and the blocked orbit, and are eventually lost after many times circulation around the torus [8]. We trace the 1 keV proton from the chaotic field line region during 200 toroidal turns of the thermal speed around the torus ($\simeq$ 15.8 msec) without collisions.

Table 3: Starting points of tracing particles. ($R_{ax} = 3.75$ m, $\varphi = 0$)

name	R	Z
Upper	3.75	$0.4373 \leq Z \leq 0.4698$
Lower	3.75	$-0.4743 \leq Z \leq -0.4373$
Outer	$4.5732 \leq R \leq 4.7891$	0
Inner	$2.7293 \leq R \leq 2.9190$	0

For the case of $R_{ax} = 3.75$m, the starting points of tracing particles are set as shown in Table 3. The initial pitch angles are given from 0 to π with step size $\pi/40$. The particle confinement characteristics in the chaotic field line region are summarized in Fig. 4.

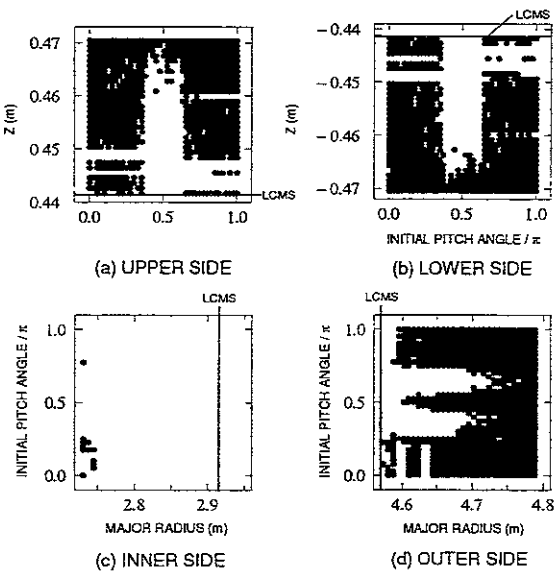

Figure 4: Relationships among initial positions and initial pitch angles in the case of $R_{ax} = 3.75$ m. Black points denote the initial conditions of lost particles. Horizontal axis is the initial pitch angle of the particle and vertical axis represents Z axis from which particles are traced in Figs. 4(a)-(b). In Figs. 4(c)-(d), horizontal axis is the initial pitch angle of the particle and vertical axis denotes R axis.

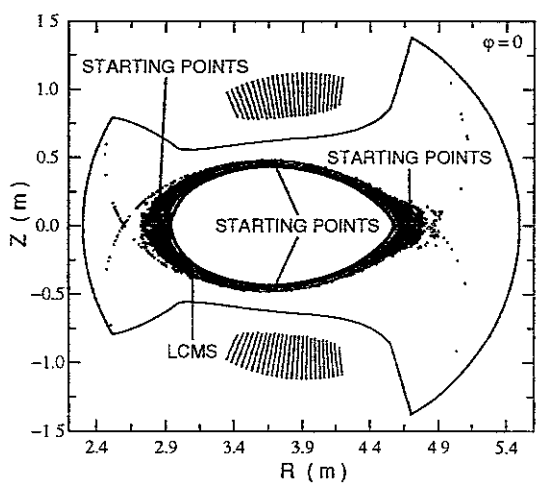

Figure 5: Poincare plots of the passing particles and the chaos orbit particles at the toroidal angle $\varphi = 0$. Black points represent the LCMS. Gray points denote the region through which particles have passed. The starting points are also shown for reference.

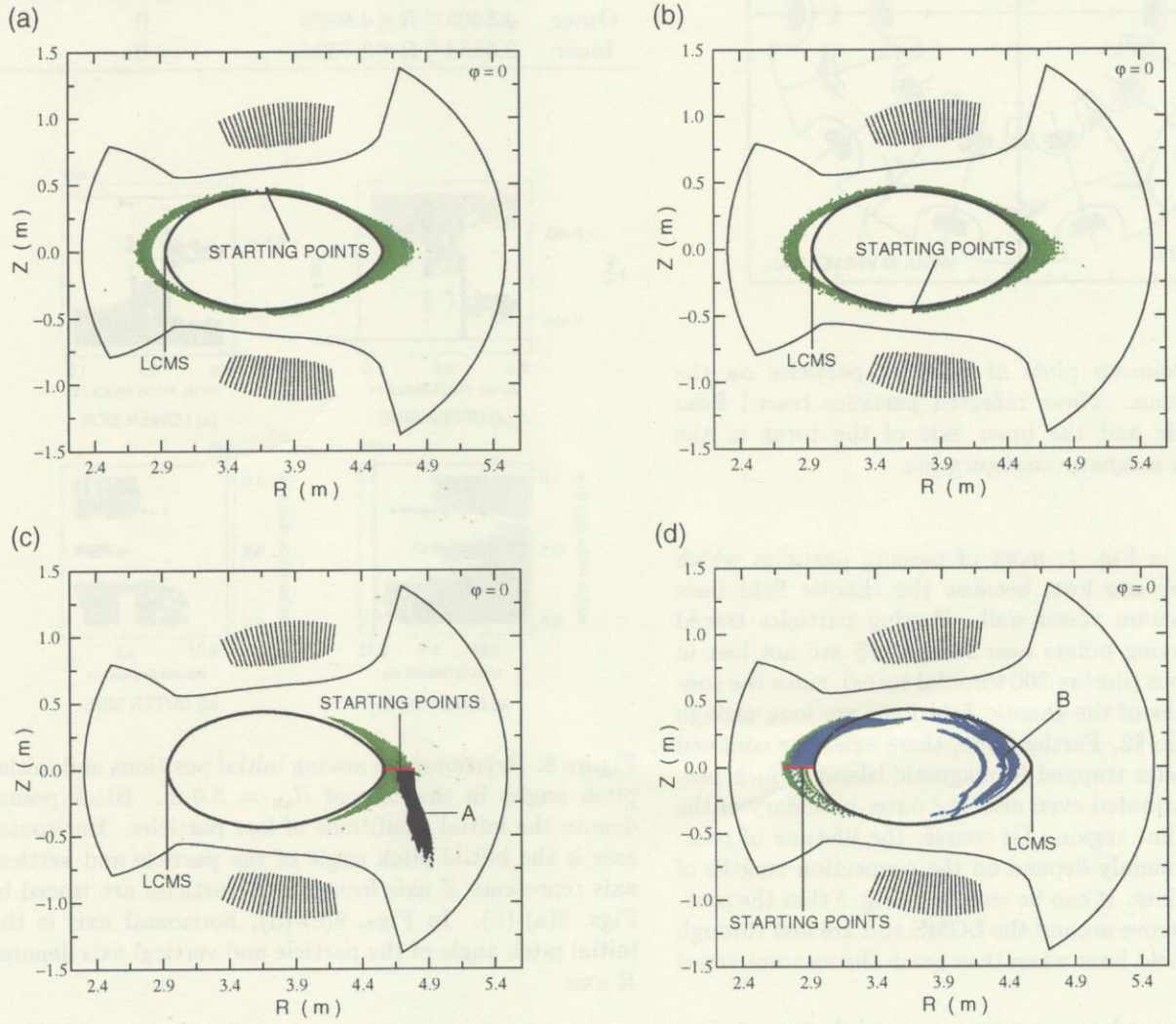

Figure 6: Poincare plot of reflected particles traced in the $R_{ax} = 3.75$ m magnetic configuration at the toroidal angle $\varphi = 0$. Particles traced from the upper, lower, outer and inner side of the torus are shown in Figs. 6(a)-(d), respectively. The starting points are also shown for reference.

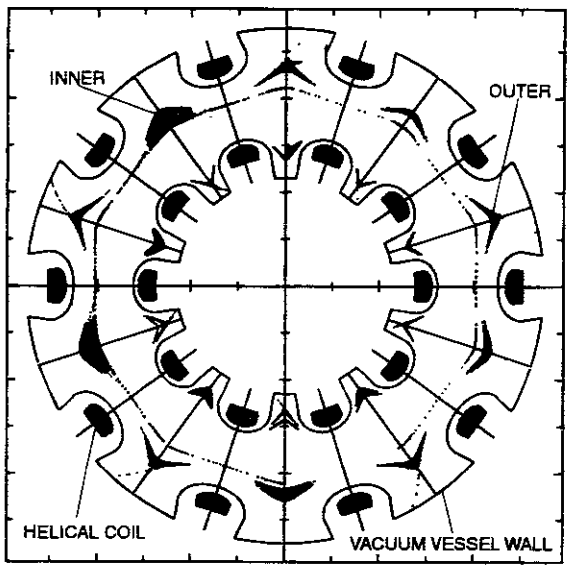

Figure 7: Poincare plots of reflected particles on the equatorial plane. These reflected particles traced from the outer side and the inner side of the torus in the $R_{ax} = 3.75$ m magnetic configuration.

As shown in Fig. 4, most of passing particles which have small $v_\perp$ are lost, because the chaotic field lines reach the vacuum vessel wall. Passing particles traced from the starting points near the LCMS are not lost in our calculations (during 200 toroidal turns), since the connection lengths of the chaotic field lines are long enough as described in §2. Furthermore, there exist the confined passing particles trapped in magnetic islands. Such particles are distributed even near the outer boundary of the chaotic field line region. Of course, the lifetime of passing particles mainly depend on the connection lengths of chaotic field lines. It can be seen from Fig. 5 that the passing particles move around the LCMS and are lost through the divertor field lines when they reach the vacuum vessel wall.

If particles circulate many times around the torus before reaching the divertor plate, they will lose their energy by collisions and radiations. Such a situation has been observed in the LHD experiment, in which the electron temperature on the divertor plate $\simeq$ 20-30eV [13]. This is preferable to the effective divertor function.

Figure 4 shows that the almost all reflected particles which start from the inner side, the upper side, and the lower side are not lost to the vacuum vessel wall. These reflected particles are trapped by the magnetic mirror in the chaotic field line region. It is also shown that there exist lost particles among the reflected particles started from the outer side in Fig. 4(d). These lost reflected particles include both the non-chaotic orbit particles and the chaotic orbit particles.

Table 4: Starting points of tracing particles ($R_{ax} = 3.6$ m, $\varphi = 0$)

name	R	Z
Upper	3.6	$0.4373 \leq Z \leq 0.4671$
Lower	3.6	$-0.4671 \leq Z \leq -0.4373$
Outer	$4.5405 \leq R \leq 4.6398$	0
Inner	$2.6154 \leq R \leq 2.7594$	0

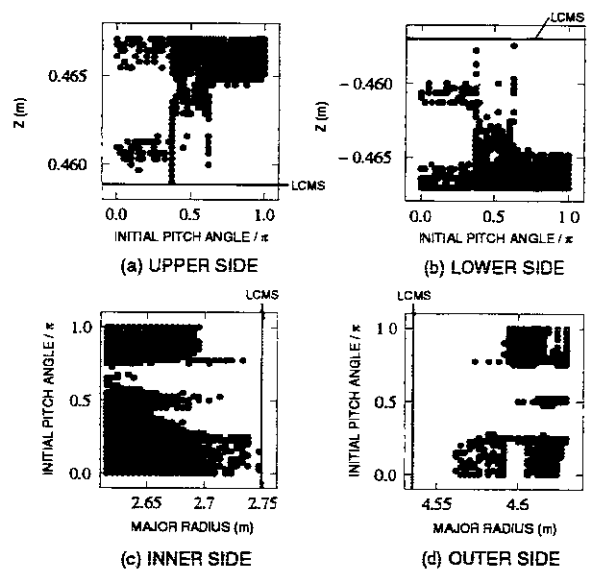

Figure 8: Relationships among initial positions and initial pitch angles in the case of $R_{ax} = 3.6$ m. Black points denote the initial conditions of lost particles. Horizontal axis is the initial pitch angle of the particle and vertical axis represents Z axis from which particles are traced in Figs. 8(a)-(b). In Figs. 8(c)-(d), horizontal axis is the initial pitch angle of the particle and vertical axis denotes R axis.

Poincare plots of reflected particles are shown in Fig. 6. It can be seen from Figs. 6(a)-(b) that reflected particles started from the upper and lower side move between the inner and outer sides of the torus and do not get into the core plasma region. As shown in Fig. 6(c), the orbit of reflected particles started from the outer side can be classified into two types. First type is the non-chaotic orbit particles that are confined in the chaotic field line region and circulate around the magnetic axis. Second type is the particles that are lost not through the divertor field lines (marked with A). As seen from Fig. 6(d), there are two types of orbits. Non-chaotic orbit particles are confined in the chaotic field line region and circulate around

the magnetic axis (Fig 7). Exceptional particles marked with B entrance and exit between the core region and the chaotic field line region. Particles-B are likely to cool down the core plasma region.

The particles confined in the chaotic field line region bring out a new concept for the peripheral plasma of LHD, i.e.. the plasma blanket. The plasma blanket could play an important role to prevent the core plasma from cooling down by cold neutrals outside the plasma.

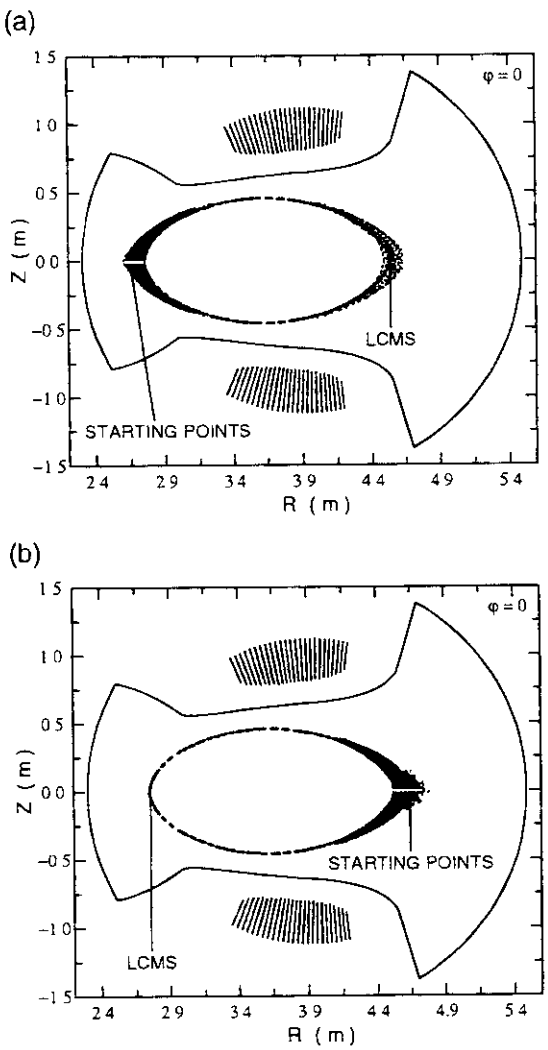

Figure 9: Poincare plot of reflected particles at the toroidal angle $\varphi = 0$. Particles traced from the inner side of torus are shown in Fig. 9(a) and particles traced from the outer side of torus are shown in Fig. 9(b). Gray points show the region through which particles have passed. The starting points are also shown for reference.

In $R_{ax} = 3.6$ m magnetic configuration, we also trace the particles from the starting points shown in Table 4. Initial pitch angles are also given from 0 to π with step size $\pi/40$. The particle confinement characteristics in the chaotic field line region are summarized in Fig. 8

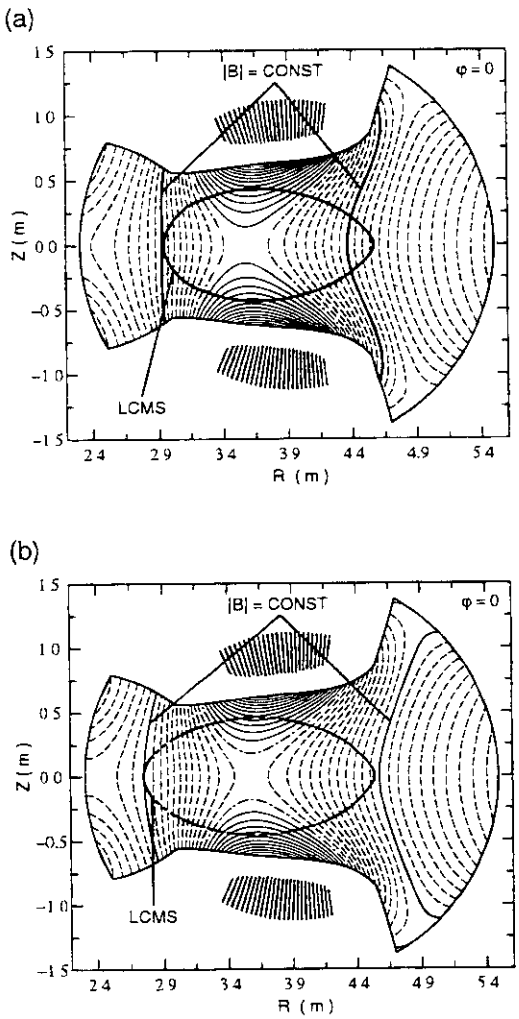

Figure 10: Contour maps of $|\boldsymbol{B}|$ in the case of $R_{ax} = 3.75$ m(a) and $R_{ax} = 3.6$ m(b). LCMS is also shown for reference.

Although the confinement characteristics in $R_{ax} = 3.6$ m configuration are almost same with that in $R_{ax} = 3.75$ m configuration, there are three differences. First is that there exists the passing particles which have the long lifetime in the upper side and the lower side. Second is that there are many lost passing particles in the inner side. Third is that the number of the lost reflected particles in the outer side is smaller than that in the $R_{ax} = 3.75$ m case. These differences between two magnetic configurations are due to the difference of the field structure of the chaotic field line region. In $R_{ax} = 3.6$ m configuration, the magnetic islands would distribute as far as the outer boundary of the chaotic field line region. Thus, there ex-

ist the passing particles which have the long lifetime in the $R_{ax} = 3.6$ m case. As shown in Fig. 2, the inner and outer side structure of the whisker field lines is inverted, comparing between two magnetic configurations. This inversion would cause the differences of the particle confinement characteristics in the inner and outer side.

The particle orbit features on the Poincare plots (Fig. 9) in the $R_{ax} = 3.6$ m configuration is also similar to that in the $R_{ax} = 3.75$ m configuration (Fig. 6). However, the orbits of the reflected particles started from the inner and outer side are different. There do not exist the particles entrancing and exiting between the core region and the chaotic field line reigon in Fig 9(a).

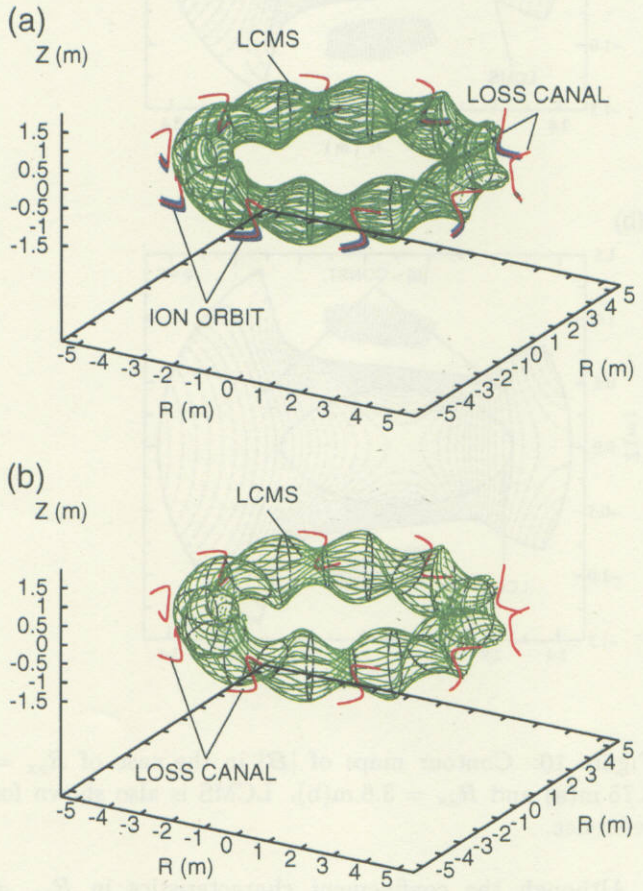

Figure 11: Loss canals in LHD. Fig. 11(a) shows the $R_{ax} = 3.75$ m magnetic configuration and Fig. 11(b) represents the $R_{ax} = 3.6$ m magnetic configuration. LCMS and the ion orbits are shown for references.

The mechanism of particles entrancing and exiting between the core region and the chaotic field line region can be explained by the differences of the field strength on the LCMS. It can been seen from Fig. 10(a) that the field strength at the inner side of the torus is stronger than that at the outer sides of torus in the $R_{ax} = 3.75$ m configuration. If the particle started from the inner side move on the LCMS, it feels weaker field. Then, by the conservation of the kinetic energy, $v_{\parallel}$ increase, so that the transition to the chaotic orbit particles would occurs. The chaotic orbit particles can entrance and exit between the core region and the chaotic field line region. On the contrary, there are no reflected particles entrancing and exiting between the core region and the chaotic field line region in the $R_{ax} = 3.6$ m configuration, because the field strength on the LCMS is almost same between the inner and outer side of torus (Fig. 10(b)). Therefore, the energy confinement in the $R_{ax} = 3.6$ m configuration would be better than that in the $R_{ax} = 3.75$ m configuration.

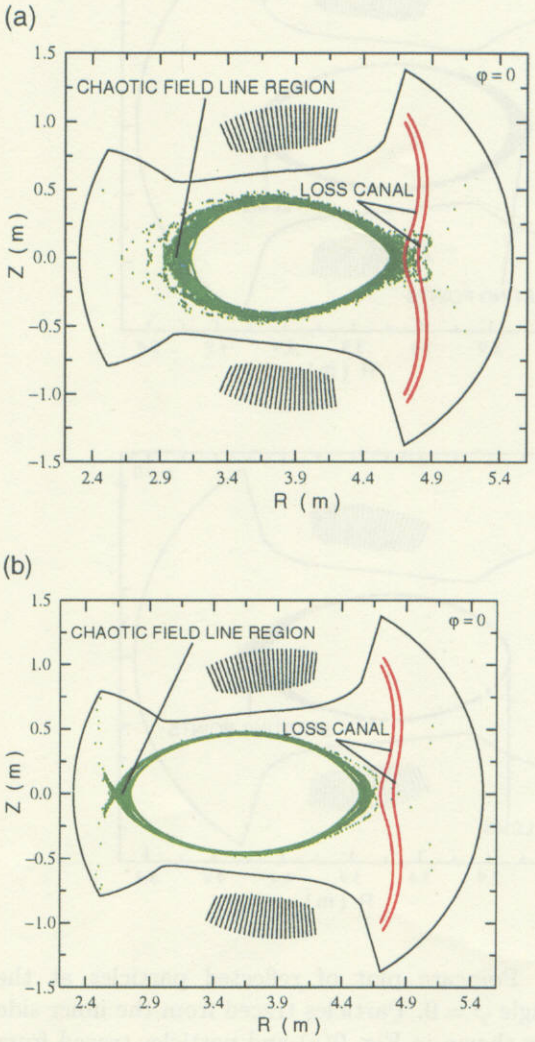

Figure 12: Positions of loss canals. Fig. 12(a) shows the $R_{ax} = 3.75$ m magnetic configuration and Fig. 12(b) showw the $R_{ax} = 3.6$ m magnetic configuration. Chaotic field line region is shown for references.

There do not also exist the particles lost not through

the divertor field line in the $R_{ax} = 3.6$ m case (Fig. 9(b)) This difference from the $R_{ax} = 3.75$m can be explained by the loss canal in the chaotic field line region. Particles-A in Fig. 6(c) are restricted to the deeply trapped particles in the magnetic mirror ($v_{\parallel} \simeq 0$). These particles should drift on the curve determined by

$$\boldsymbol{B} \cdot \nabla B = 0, \tag{1}$$

and

$$|\boldsymbol{B}| = \text{constant}. \tag{2}$$

By the numerical analysis of the $R_{ax} = 3.75$ m magnetic configuration, it is found that there exists the curves connecting the chaotic field line region and the vacuum vessel wall (Fig 11(a)). Particles-A is lost through these curves called the loss canals. The loss canals is also found in the $R_{ax} = 3.6$ m case (Fig 11(b)), with almost same configuration to the $R_{ax} = 3.75$ m case. The difference of the particle orbits is due to the positions of the loss canals. As shown in Fig. 12(b), the loss canals are located outside the chaotic field line region in the $R_{ax} = 3.6$ m configuration. Thus, in Fig 9(b), there exist no particles lost through the loss canals in the $R_{ax} = 3.6$ m case.

4 Summary and Discussion

The magnetic field structure and the particle orbit in the periphery of LHD have been studied numerically.

The border of the chaotic field line region has been determined precisely. It has been found that the core plasma region in $R_{ax} = 3.6$ m magnetic configuration is slightly bigger than that of $R_{ax} = 3.75$ m magnetic configuration. On the contrary, the chaotic field line region in $R_{ax} = 3.6$ m magnetic configuration is thicker than that of $R_{ax} = 3.75$ m magnetic configuration. The connection lengths of the divertor field lines have been also studied. It has been found that the chaotic field lines in LHD have sufficiently long connection lengths ($\gtrsim$20km) in the both magnetic configuration.

The particles confined in the chaotic field line region consist of two groups. Group-1 are the passing particles that have long lifetime because of the extremely long connection length of the chaotic field line. Although passing particles in the chaotic field line region are eventually lost, such particles are expected to reduce the thermal load to the divertor plate by collision or bremsstrahlung. Group-2 are the non-chaotic orbit particles that are confined by the magnetic mirror in the chaotic field line region. Group-2 particles are perfectly confined in the chaotic field line region in the case of no collisions. The basic period length of reflected particle motion is small compared with that of the passing particle motion. Thus, reflected particles can manifest strong adiabaticity and be confined in collision less case [9]. Group-1 and group-2 particles are expected to be the plasma blanket that protects the core plasma from cooling down by neutrals outside the plasma.

It has been also found that there are two types exceptional reflected particles in $R_{ax} = 3.75$ m case. First type called particles-A is the particles lost not through the divertor field line Second type called particles-B is the particles entrancing and exiting between the core plasma region and the chaotic field line region. The mechanisms of the exceptional particles have been also studied by the magnetic structure analysis. Particles-A, deeply trapped by the magnetic mirror, are lost through the loss canals which are determined by the cross-lines of $|\boldsymbol{B}| = $ const. plane and $\boldsymbol{B} \cdot \nabla B = 0$ plane. The mechanism of the particles-B which entrance and exit between the core region and the chaotic field line region can be explained by the differences of the field strength on the LCMS and the conservation of the kinetic energy. It would be one of the factors of the improvement of the plasma confinement that there do not exist the particles-B in the $R_{ax} = 3.6$ m configuration.

If the resonance position of the electron cyclotron heating (ECH) or the ion cyclotron resonance frequency (ICRF) heating is placed at loss canals, electrons or ions can be removed selectively from the chaotic field line region. As a result, the peripheral potential would be able to be controlled. These active potential control method are expected to improve the core plasma confinement. In addition, such a peripheral potential control should be useful to remove the ^{4}He ash produced by D-T or p-^{11}B fusion reaction, if the ICRF frequency is set equal to the ^{4}He cyclotron frequency. However, the active potential control and the ^{4}He ash removal methods cannot be used in $R_{ax} = 3.6$ m configuration, since the loss canals are located outside the chaotic field line region.

Particles having $v_{\parallel} \simeq 0$ move along the cross-lines of $|\boldsymbol{B}| = $ const. plane and $\boldsymbol{B} \cdot \nabla B = 0$ plane. These cross-lines from the chaotic field line region are shown in Fig. 13. This implies that the deeply trapped particles are confined in the weak magnetic field region between helical coils and circulate around the magnetic axis with the same pitch of the rotation of helical coils. There are a cross-line which entrances and exits between the core plasma region and the chaotic field line region and the cross-lines located in the chaotic field line region, as shown in Fig. 13. Particles move along these cross-lines are confirmed in our particle orbit computations.

In this paper, the effects of the collisions between particles are not considered. Of cause, collisions have the important effects on the particle orbit. A major effect of collisions on the particle orbit in the chaotic field line region is the pitch-angle scattering. By the pitch-angle scattering, the transition between passing particles and reflected particles occurs. This transition would not have a serious effect on the plasma confinement in the chaotic

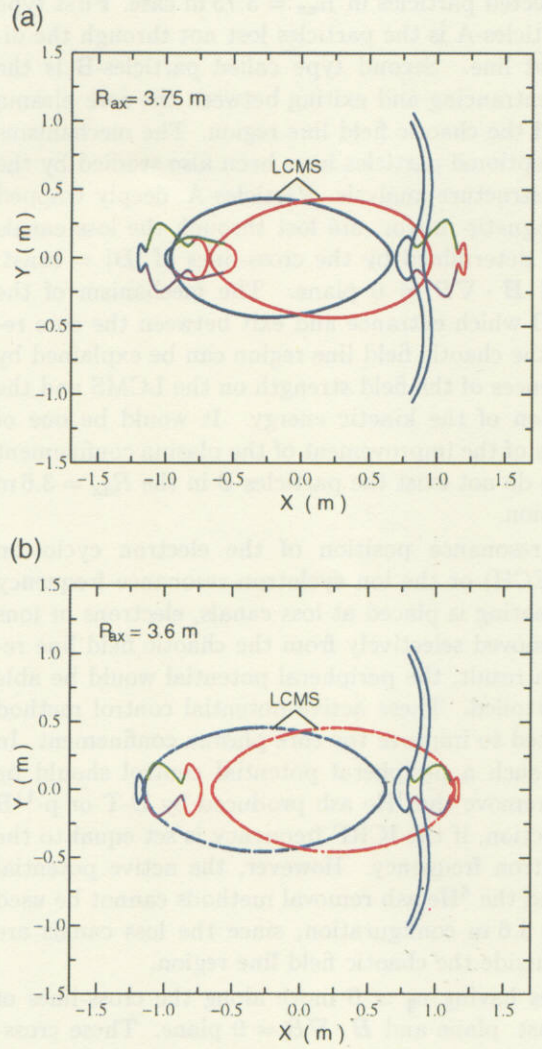

Figure 13: Cross-lines of $|\boldsymbol{B}| =$ const. plane and $\boldsymbol{B}\cdot\nabla B = 0$ plane in the chaotic field line region. Fig. 13(a) shows the $R_{\rm ax} = 3.75$ m magnetic configuration and Fig. 13(b) shows the $R_{\rm ax} = 3.6$ m magnetic configuration. X shows the direction to the major axis of the magnetic surface and Y shows the direction to the minor axis in the rotating helical coordinates [8]. The range of toroidal angle φ is shown by colors of points,
Blue: $(8n-1)\pi/20 < \varphi < (8n+1)\pi/20$,
Green: $(8n+1)\pi/20 < \varphi < (8n+3)\pi/20$,
Red: $(8n+3)\pi/20 < \varphi < (8n+5)\pi/20$,
Purple: $(8n+5)\pi/20 < \varphi < (8n+7)\pi/20$
$(n = 0, 1, \ldots, 4)$.

field line region, because both passing and reflected particles are well-confined in the chaotic field line region.

We have not considered the heat transport, the particle diffusion, the electric field and the charge exchange effect. These effects on the peripheral plasma are very important. Further analysis that includes these effects will be carried out in the future.

Acknowledgements

We are grateful to Prof. T. Yamashina (Sapporo International University) and Prof. M. Itagaki (Hokkaido University) for continuous encouragement. We are also indebted to Mr. T. Nagaura (NEC Soft, Ltd.) and Mr. Y. Itoh (Hokkaido University) for their helpful advice. We thank all members of the LHD experimental group and the theory and data analysis division (National Institute for Fusion Science (NIFS)) for valuable discussions.

References

[1] M. Fujiwara: J. Plasma Fusion Res. **74** (1998) suppl. 10 [in Japanese].

[2] M. Wakatani: *Stellarator and Heliotron device.* (Oxford University Press, New York, 1998) §6.

[3] A. Gibson and J. B. Taylor: Phys. Fulids **10** (1967) 2653.

[4] A. Gibson and D. W. Mason: Plasma Phys. **11** (1969) 121.

[5] K. Hanatani and F. -P. Pennigsfeld: Nucl. Fusion **32** (1992) 1769.

[6] H. Sanuki, J. Todoroki and T. Kamimura: Phys. Fluids B **2** (1990) 2155.

[7] R. H. Fowler, R. N. Morris, J. A. Rome, and K. Hanatani: Nucl. Fusion **30** (1990) 997.

[8] T. Watanabe, A. Ishida, and T. Hatori: Kakuyugo-Kenkyu **68** (1992) 298 [in Japanese].

[9] L. D. Landau and E.M.Lifshitz: *Mechanics and Electrodynamics.* (Pergamon Press, Oxford, 1976) 108.

[10] H. Akao: J. Phys. Soc. Jpn. **59** (1990) 1633.

[11] N. Ohyabu, A. Komiri, K. Kawakita, O. Kaneko, H. Yamada, O. Motojima and LHD Experimental Group: J. Plasma Fusion Res. **76** (2000) 425 [in Japanese].

[12] C. S. Pitcher and P. C. Stangeby: Plasma Phys. Control. Fusion. **36** (1997) 779.

[13] S Masuzaki, T Morisaki, R. Sakamoto, H. Suzuki, A Komori, N. Ohyabu, B. Peterson, K. Narihara, I. Yamada, Y. Matsumoto, T. Watanabe, O. Motojima and LHD experimental group: 26th European Physical Society Conference on Controlled Fusion and Plasma Physics. (1999).

Recent Issues of NIFS Series

NIFS-687 T Kuroda and H Sugama,
Effects of Multiple-Helicity Fields on Ion Temperature Gradient Modes Apr 2001

NIFS-688 M Tanaka,
The Origins of Electrical Resistivity in Magnetic Reconnection Studies by 2D and 3D Macro Particle Simulations Apr 2001

NIFS-689 A Maluckov, N Nakajima, M Okamoto, S Murakami and R Kanno,
Statistical Properties of the Neoclassical Radial Diffusion in a Tokamak Equilibrium Apr 2001

NIFS-690 Y Matsumoto, T Nagaura, Y Itoh, S-I Oikawa and T Watanabe
LHD Type Proton-Boron Reactor and the Control of its Peripheral Potential Structure Apr 2001

NIFS-691 A Yoshizawa, S -I Itoh, K Itoh and N Yokoi,
Turbulence Theories and Modelling of Fluids and Plasmas Apr 2001

NIFS-692 K Ichiguchi, T Nishimura, N Nakajima, M Okamoto, S -i Oikawa, M Itagaki,
Effects of Net Toroidal Current Profile on Mercier Criterion in Heliotron Plasma Apr 2001

NIFS-693 W Pei, R Horiuchi and T Sato,
Long Time Scale Evolution of Collisionless Driven Reconnection in a Two-Dimensional Open System Apr 2001

NIFS-694 L N Vyacheslavov, K Tanaka, K Kawahata,
CO2 Laser Diagnostics for Measurements of the Plasma Density Profile and Plasma Density Fluctuations on LHD Apr 2001

NIFS-695 T Ohkawa,
Spin Dependent Transport in Magnetically Confined Plasma May 2001

NIFS-696 M Yokoyama, K Ida, H Sanuki, K Itoh, K Narihara, K Tanaka, K Kawahata, N Ohyabu and LHD experimental group
Analysis of Radial Electric Field in LHD towards Improved Confinement May 2001

NIFS-697 M Yokoyama, K Itoh, S Okamura, K Matsuoka, S -I Itoh,
Maximum-J Capability in a Quasi-Axisymmetric Stellarator May 2001

NIFS-698 S-I Itoh and K Itoh,
Transition in Multiple-scale-lengths Turbulence in Plasmas May 2001

NIFS-699 K Ohi, H Naitou, Y Tauchi, O Fukumasa,
Bifurcation in Asymmetric Plasma Divided by a Magnetic Filter May 2001

NIFS-700 H Miura, T Hayashi and T Sato,
Nonlinear Simulation of Resistive Ballooning Modes in Large Helical Device June 2001

NIFS-701 G Kawahara and S Kida,
A Periodic Motion Embedded in Plane Couette Turbulence June 2001

NIFS-702 K Ohkubo,
Hybrid Modes in a Square Corrugated Waveguide June 2001

NIFS-703 S -I Itoh and K Itoh,
Statistical Theory and Transition in Multiple-scale-lengths Turbulence in Plasmas June 2001

NIFS-704 S Toda and K Itoh,
Theoretical Study of Structure of Electric Field in Helical Toroidal Plasmas June 2001

NIFS-705 K Itoh and S-I Itoh,
Geometry Changes Transient Transport in Plasmas June 2001

NIFS-706 M Tanaka and A Yu Grosberg
Electrophoresis of Charge Inverted Macroion Complex Molecular Dynamics Study July 2001

NIFS-707 T-H Watanave, H Sugama and T Sato
A Nondissipative Simulation Method for the Drift Kinetic Equation July 2001

NIFS-708 N Ishihara and S. Kida,
Dynamo Mechanism in a Rotating Spherical Shell Competition between Magnetic Field and Convection Vortices July 2001

NIFS-709 LHD Experimental Group,
Contributions to 28th European Physical Society Conference on Controlled Fusion and Plasma Physics (Madeira Tecnopolo, Funchal, Portugal, 18-22 June 2001) from LHD Experiment July 2001

NIFS-710 V Yu. Sergeev, R K Janev, M J Rakovic, S. Zou, N Tamura, K.V Khlopenkov and S. Sudo
Optimization of the Visible CXRS Measurements of TESPEL Diagnostics in LHD. Aug 2001

NIFS-711 M Bacal, M Nishiura, M Sasao, M Wada, M Hamabe, H Yamaoka,
Effect of Argon Additive in Negative Hydrogen Ion Sources, Aug 2001

NIFS-712 K Saito, R. Kumazawa, T Mutoh, T Seki, T Watari, T Yamamoto, Y Torii, N Takeuchi C Zhang, Y Zhao, A Fukuyama, F Shimpo, G Nomura, M Yokota, A Kato, M Sasao, M Isobe, A V Krasilnikov, T Ozaki, M Osakabe, K Narihara, Y Nagayama, S Inagaki, K Itoh, T Ido, S. Morita, K Ohkubo, M Sato, S Kubo, T Shimozuma, H Idei, Y Yoshimura, T Notake, O Kaneko, Y Takeiri, Y. Oka, K Tsumori K Ikeda A Komori, H Yamada, H Funaba, K Y Watanabe, S Sakakibara, R Sakamoto, J Miyazawa, K. Tanaka, B J Peterson, N Ashikawa, S Murakami, T Minami, M Shoji, S Ohdachi, S Yamamoto, H Suzuki, K Kawahata, M Emoto, H Nakanishi, N Inoue, N Ohyabu, Y Nakamura, S Masuzaki, S Muto, K Sato, T Morisaki, M Yokoyama, T Watanabe, M Goto, I Yamada, K. Ida, T Tokuzawa, N Noda, K Toi S Yamaguchi, K Akaishi, A Sagara, K Nishimura, K Yamazaki, S Sudo, Y Hamada, O Motojima, M Fujiwara,
A Study of High-Energy Ions Produced by ICRF Heating in LHD. Sep 2001

NIFS-713 Y Matsumoto, S -I Oikawa and T Watanabe
Field Line and Particle Orbit Analysis in the Periphery of the Large Helical Device, Sep 2001